# Specific heat and upper critical fields in KFe₂As₂ single crystals

M. Abdel-Hafiez,[*] S. Aswartham, S. Wurmehl, V. Grinenko, C. Hess, S.-L. Drechsler, S. Johnston,
A. U. B. Wolter, and B. Büchner

*Leibniz-Institute for Solid State and Materials Research, (IFW)-Dresden, D-01171 Dresden, Germany*

H. Rosner

*Max-Planck-Institute for Chemistry of Solid Materials (CPfS), D-01187 Dresden, Germany*

L. Boeri

*Max-Planck-Institute for Solid State Research, Heisenbergstrasse 1, D-70569 Stuttgart, Germany*

We report low-temperature specific heat measurements for high-quality single crystalline KFe₂As₂ ($T_c \approx$ 3.5 K). The investigated zero-field specific heat data yields an unusually large nominal Sommerfeld coefficient, $\gamma_n = 94(3)$ mJ/mol K², which is, however, affected by extrinsic contributions as evidenced by a sizable residual linear specific heat and various theoretical considerations, including an analysis of Kadowaki-Woods relations. These results indicate that KFe₂As₂ should be classified as a weakly or intermediately coupled superconductor with a total electron-boson coupling constant $\lambda_{tot} \sim 1$ (including a calculated weak electron-phonon coupling $\lambda_{ph} = 0.17$). From specific heat and ac susceptibility studies in external magnetic fields the magnetic phase diagram is also constructed. We confirm the high anisotropy of the upper critical fields $\mu_0 H_{c2}(T)$, ranging from a factor of 5 near $T_c$ to a slightly reduced value around 4.5 approaching $T = 0$ for fields $B \parallel ab$ and $\parallel c$ and show that their ratio slightly exceeds the mean mass anisotropy of 4.4 derived from our full-relativistic local-density-approximation band structure calculations, also in accord with recent preliminary penetration depth data by Eskildsen *et al.* [Eskildsen, Forgan, and Kawano-Furukawa, Rep. Prog. Phys. **74**, 124504 (2011)] near 4. Its slight reduction when approaching $T = 0$ is not a consequence of Pauli limiting as in less perfect samples but points likely to a multiband effect. We also report irreversibility field data obtained from ac susceptibility measurements. The double-maximum in the $T$ dependence of its imaginary part for fields $B \parallel c$ indicates a peak effect in the $T$ dependence of critical currents.

## I. INTRODUCTION

Since the discovery of superconductivity (SC) in an electron-doped LaFeAsO (La-1111) compound with a superconducting transition temperature $T_c \sim 26$ K,[1] iron pnictides are of great interest in fundamental condensed matter physics due to their large variety of structural, magnetic, and electronic properties. In order to understand the nature of superconductivity in Fe pnictides, a huge amount of theoretical and experimental studies have been performed but, nevertheless, many questions remain unanswered, such as the symmetry of the order parameter and the pairing mechanism, as well as their relation to the magnetic properties. In this situation, low-$T$ specific heat and magnetic susceptibility measurements are helpful since they provide insight into many-body physics via the renormalization of such physical quantities as the Sommerfeld coefficient $\gamma_{el}$ (a measure of the renormalized density of states), the irreversibility field $H_{irr}$, the upper critical field $H_{c2}$, its anisotropy, and so on. All are important factors that affect superconducting and the normal-state properties. In particular, they can shed light on the Fermi surface topology and other relevant aspects of the electronic structure. To address the role of magnetism in the formation of the superconducting state studying the heavily hole-doped KFe₂As₂ (K-122) is worthwhile due to its distinctive characteristics with respect to other stoichiometric 122 and 1111 Fe-pnictide compounds: (i) there is no static magnetic ordering in the sense of an ordinary spin-density

wave (SDW) nor an orthorhombic structural transition.[2,3] (ii) Superconductivity occurs in relatively dirty samples near 2.8 K[4] and increases up to 3.5 to 3.7 K[3] in cleaner high-quality single crystals. (iii) Remarkably, no nesting of the Fermi surface has been detected, in contrast to, e.g., Ba₀.₆K₀.₄Fe₂As₂.[5,6] However, a neutron-scattering study of heavily hole-doped superconducting KFe₂As₂ revealed well-defined low-energy incommensurate spin fluctuations at $q = [\pi(1 \pm 2\delta),0]$ with $\delta = 0.16$.[7] This differs from the previously observed commensurate antiferromagnetism (AFM) of electron-doped $A$Fe₂As₂ ($A$ = Ba, Ca, or Sr) at low energies. Additionally, de Haas-van Alphen[8] and cyclotron resonance[9] studies of KFe₂As₂ revealed a strong mass enhancement of the quasiparticles. K-122 exhibits a very large anisotropy as compared with less hole-doped members of the 122 family and other Fe-pnictide and chalgogenide superconductors.[10] After naturally more electronically anisotropic 1111 and Tl₁₋ᵧRbᵧFe₁₋δSe₂ with $y \sim 0.4, \delta \sim 0.3$ superconductors showing only slightly larger or comparable slope anisotropies of $\sim$5 to 6, K-122 belongs to the most anisotropic pnictides.[11] A complete understanding of their critical field slopes near $T_c$ is still missing due to the complex interplay of pair-breaking impurities and the symmetry of the superconducting order parameter.[12]

The magnetic phase diagram of KFe₂As₂ has been studied via resistivity measurements on single crystals,[4] however, its determination using thermodynamic bulk techniques on single crystalline material is lacking up to now.[13,14] In this context,

we note the recent discovery of a very high surface upper critical field $H_{c3}$ with $H_{c3}(T)/H_{c2}(T) \sim 4.4$ for the external field $\parallel$ to the $ab$ plane in $K_{0.73}Fe_{1.68}Se_2$.[15] For that direction, nucleation starts at the much higher $H_{c3}$, and resistivity and/or ac susceptibility measurements might, in principle, lead to confusion between $H_{c2}$ and $H_{c3}$, and overestimates for the anisotropy of the upper critical fields. Hence, for this geometry, specific heat studies of high-quality single crystals are mandatory to address their bulk anisotropy.

In this work we present low-$T$ specific heat and ac magnetization studies on high-quality superconducting $KFe_2As_2$ single crystals. These crystals have a larger $T_c$ and a much higher residual resistivity ratio as compared to the first single crystals used for an upper critical field study for $KFe_2As_2$ by Terashima *et al.*,[4] where a large anisotropy ratio of the upper critical fields, as well as for the electric resistivity perpendicular and parallel to the $ab$ plane, have been reports. The obtained data are analyzed within the framework of various theoretical approaches. In particular, we found good agreememt with the electron mass anisotropy derived from density funtional theory (DFT) considering in- and out-of-plane plasma frequencies and Fermi velocities.

## II. EXPERIMENTAL

Single crystals of $KFe_2As_2$ have been grown using a self-flux method with K:Fe:As in the molar ratio of 1:5:5. All preparation steps such as weighing, mixing, grinding, and storage were carried out in an Ar-filled glove box. As a first step, the appropriate amounts of the precursor materials FeAs and $Fe_2As$ were thoroughly ground in an agate mortar. Second, the exact amount of weighed KAs was deposited at the bottom of an alumina crucible, where on top of it the well-ground mixture was placed carefully and, finally, sealed in a niobium crucible. The sealed crucible assembly was placed in a vertical furnace, heated up to 1373 K, and cooled down to 1023 K at a rate of 2 K/h. Finally, the furnace was cooled very quickly from 1023 K to room temperature. All crystals were grown with layerlike morphology and they were found to be quite easy to cleave along the $ab$ plane. The quality of the grown single crystals was assessed by complementary techniques. Several samples were examined with a scanning electron microscope (SEM Philips XL 30) equipped with an electron microprobe analyzer for a semiquantitative elemental analysis using the energy dispersive x-ray (EDX) mode. The composition was estimated by averaging over several different points of the plateletlike single crystals and was found to be consistent and homogeneous with a 122 structure within the instrumental error bars. Typical crystal sizes with a rectangular shape were about $1.2 \times 0.5$ mm$^2$ and with a thickness of 50 $\mu$m along the $c$ axis. The two crystals chosen for the specific heat measurements exhibited rather similar $T_c$ values (see the insets of Figs. 2 and 8).

Low-temperature specific heat and ac magnetization have been determined using a Physical Property Measurement System (PPMS from Quantum Design). The specific heat data were measured using a relaxation technique. For the measurements with $H \parallel ab$, a small copper block has been used to mount the sample on the specific heat puck. The heat capacity of the copper block was determined in a separate measurement and its value was subtracted from the raw data of $KFe_2As_2$.

## III. RESULTS AND DISCUSSIONS

### A. ac magnetization measurements

Figure 1 depicts the $T$ dependence of the volume ac susceptibilities ($\chi'_v$ and $\chi''_v$) of our $KFe_2As_2$ single crystal. The measurements were done in an ac field with an amplitude $B_{ac} = 5$ Oe, a frequency $f = 1$ kHz, and dc fields up to 5 T parallel to the $ab$ plane [as shown in Fig. 1(a)] and parallel to the $c$ axis [in Fig. 1(b)]. Special care has been taken to correct the magnetization data for demagnetization effects, where the demagnetization factor has been estimated based on the crystal dimensions.[16] The ac susceptibility measurements can be used for an investigation of the flux dynamics in superconductors.[17–19] The imaginary part $\chi''_v$ is related with the energy dissipation in a sample and the real part $\chi'_v$ is related with the amount of screening. Both these functions depend on the ratio between skin depth $\delta_s$ and the sample dimension $L$ in the direction of the flux penetration. In the normal state $\delta_s \sim (\rho_n/f)^{0.5}$, where $\rho_n$ is the normal-state resistivity and $f$ is the frequency. In the superconducting state the skin depth $\delta_s \propto \lambda_L$ in an external magnetic field above the first critical
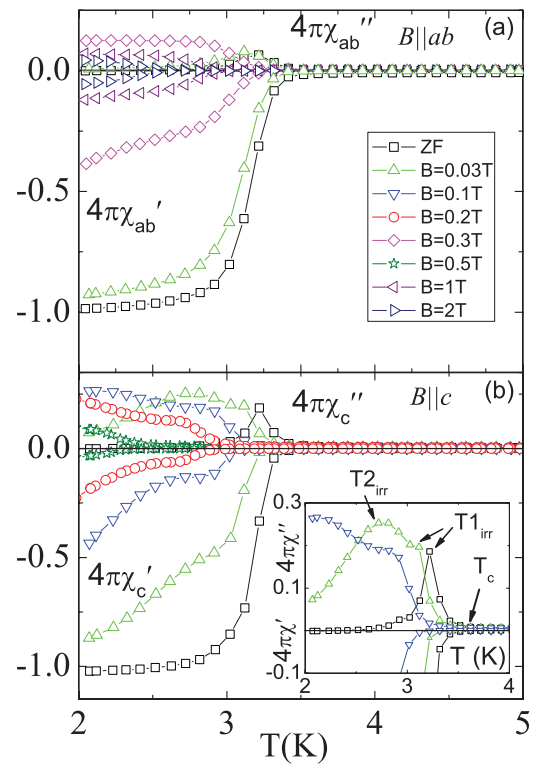


FIG. 1. (Color online) (a) The $T$ dependence of the complex ac susceptibility components $4\pi\chi'_v$ and $4\pi\chi''_v$ of $KFe_2As_2$ has been measured in an ac field with an amplitude of 5 Oe and a frequency of 1 kHz on warming in different dc magnetic fields after cooling in zero magnetic field with (a) $B \parallel ab$ and (b) $B \parallel c$. The sharp superconducting transition with $\sim 100\%$ superconducting volume fraction indicates the bulk nature of superconductivity and the high quality of our crystal. The inset shows the criteria used to obtain $T_c$ and $T_{irr}$; for details see the text.

field $H_{c1}$, where $\lambda_L$ is the London penetration depth. For magnetic fields above $H_{c1}$, $\delta_s \propto L_B$, where $L_B \sim B_{ac}/J_c$ is the Bean's penetration depth and $J_c$ is the critical current density. In general, if $L \ll \delta_s$ an ac field completely penetrates the sample and, thus, the susceptibility is small. In the opposite case, if $L \gg \delta_s$, most of the sample volume is screened, therefore, $4\pi\chi'_v = -1$ and $\chi''_v \rightarrow 0$. In accordance with this the ac susceptibility data measured at low $T$ confirm the bulk superconductivity of our KFe$_2$As$_2$ single crystal (Fig. 1); $T_c \sim 3.6(1)$ K has been extracted from the bifurcation point between $\chi'_v$ and $\chi''_v$ as shown in the inset of Fig. 1(b). This point is related with a change in the linear resistivity due to the superconducting transition. It can be also used for the determination of the $T$ dependence of the upper critical field $H_{c2}$ from ac susceptibility data measured at various dc fields.[17]

At $T < T_c$ the function $\chi''_v$ increases with decreasing temperature and some value of $T = T_{irr}$ where $(L \sim \delta_s)$ $\chi''_v$ has a maximum (see Fig. 1). The above discussed Bean's approximation predicts that the $T$ dependence of the peak in $\chi''_v$ follows the $T$ dependence of the critical current density $J_c$. Thus, one might relate $T_{irr}$ with an irreversibility temperature and use its dc field dependence to obtain the irreversibility field $H_{irr}$.[19] However, we remind the reader that $H_{irr}$ defined this way is not the "true" irreversibility field since by definition $H_{irr}$ is the field at which $J_c = 0$. From this point of view, it is better to use dc magnetization data to obtain the irreversibility line. In general, we observed a rough agreement between $H_{irr}$ obtained from dc and ac susceptibility data, but the large value and the strong $T$ dependence of the normal-state dc susceptibility lead to a large uncertainty in determination of the $H_{irr}$. Therefore, to obtain the irreversibility line we have used ac susceptibility data. (The dc susceptibility data will be presented elsewhere).[20] Thus, with some caution, we relate the maximum in the $T$ dependence of $\chi''_v$ to $T_{irr}$. It can be seen in Fig. 1(b) that at nonzero $B_{dc} \| c$ the single maximum in $\chi''_v$ splits into two features at $T1_{irr}$ and $T2_{irr}$. Therefore, for $B_{dc} \| c$ we defined two different "irreversibility" fields, $H1_{irr}$ and $H2_{irr}$. The $T$ dependence of these fields is plotted in Fig. 6.

### B. Specific heat studies

Figure 2 shows the $T$ dependence of the zero-field specific heat measured down to 0.4 K. A clear sharp anomaly was observed near 3.5 K, in agreement with the magnetization data. In order to determine the zero-field normal-state Sommerfeld coefficient $\gamma_n$, the specific heat can be plotted for $T > T_c$ as $c_p/T$ versus $T^2$ following

$$c_p = \gamma_n T + \beta_3 T^3 + \beta_5 T^5 + \cdots, \quad (1)$$

with $\gamma_n$ and $\beta_3$, $\beta_5$ as the nominal electronic and lattice coefficients, respectively. The values obtained for our KFe$_2$As$_2$ sample are $\gamma_n = 94(3)$ mJ/mol K$^2$, $\beta_3 = 0.79$ mJ/mol K$^4$, and $\beta_5 = 6.09 \times 10^{-4}$ mJ/mol K$^6$. Our $\gamma_n$ value compares very well with $\gamma_n = 93$ mJ/mol K$^2$ reported in Ref. 21. From the relation for the Debye temperature, $\theta_D = (12\pi^4 RZ/5\beta_3)^{1/3}$, where $R$ is the molar gas constant and $Z = 5$ is the number of atoms per formula unit, we obtain $\theta_D = 214$ K.
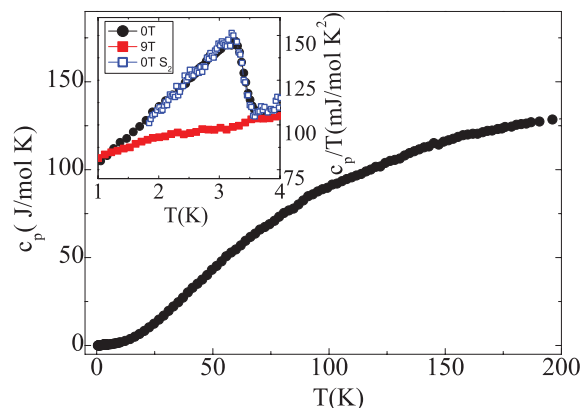


FIG. 2. (Color online) The $T$ dependence of the zero-field specific heat of KFe$_2$As$_2$ for 400 mK $\leqslant T \leqslant$ 200 K. The inset shows $c_p/T$ versus $T$ of our 0-T and 9-T data together with the zero-field of another sample (S$_2$) shows the same $T_c(H)$ behavior down to 1.8 K.

Notice the large value of $\gamma_n$ KFe$_2$As$_2$ as compared to other stoichiometric and nonstoichiometric 122 compounds, or to any other superconducting iron pnictide or chalcogenide, reported so far to the best of our knowledge. The low values of $\gamma_n$ for BaFe$_2$As$_2$ and SrFe$_2$As$_2$ are not surprising since large parts of its Fermi surface are gapped due to the well-known magnetic spin density wave (SDW) transition at high temperatures. In this light, a comparison with a hole-doped system where the SDW transitions are suppressed is more meaningful. For instance, for the closely related, nearly optimal hole-doped systems Ba$_{0.68}$K$_{0.32}$Fe$_2$As$_2$ ($T_c = 38.5$ K),[22] Ba$_{0.6}$K$_{0.4}$Fe$_2$As$_2$ ($T_c = 36.5$ K),[23] or Ba$_{0.65}$K$_{0.35}$Fe$_2$As$_2$ ($T_c = 29.4$ K),[24] the Sommerfeld parameters $\gamma_n = 50.0$, 63.3, and 57.5 mJ/mol K$^2$, respectively, have been reported. In view of their much-higher $T_c$ values, often attributed to strong-coupling corrections with $\lambda \sim 2$[22] (spin fluctuation mediated interband coupling) and a comparable bare value of $\gamma_b \sim 10$ mJ/mol K$^2$ (derived from DFT-band structure calculations), the unusual large value for KFe$_2$As$_2$ reported above provides a surprising puzzle. However, the puzzling difference in $\gamma_n$ can be somewhat reduced if there is an essential *extrinsic* contribution to the system of intinerant charge charriers, e.g., due to defect states with low-energy excitations.[20] To be consistent with such an analysis we are forced to assume that KFe$_2$As$_2$ is *not* in the strong-coupling limit, which seems to be natural in view of its low $T_c$ value (to be discussed in future work within the framework of Eliashberg theory).

The general situation, independent of the strength of the electron-boson coupling regime and the symmetry of the order parameter, is plotted in Figs. 3 and 4 using the calculated DFT values $\gamma_b$[22,25,26] as convenient bare values, whereby the high-energy renormalization $\eta = 2.7$ as derived from the calculated DFT plasma frequencies of 2.58 eV[25] and 2.56 eV[26,27] and the expected experimental unscreened plasma frequency of about 1.55 eV have been taken into account.[28] The two strong-coupling points shown in Fig. 4 would give much too high a $T_c$ in a quasiclean situation. In order to reproduce the experimental $T_c$ value, a very strong pair-breaking mechanism would have to be assumed and K122 would be expected to be located on the universal curve $\Delta c_{el} \propto T_c^3$ as established for many iron pnictides.[29] Since this is *not* the case, a
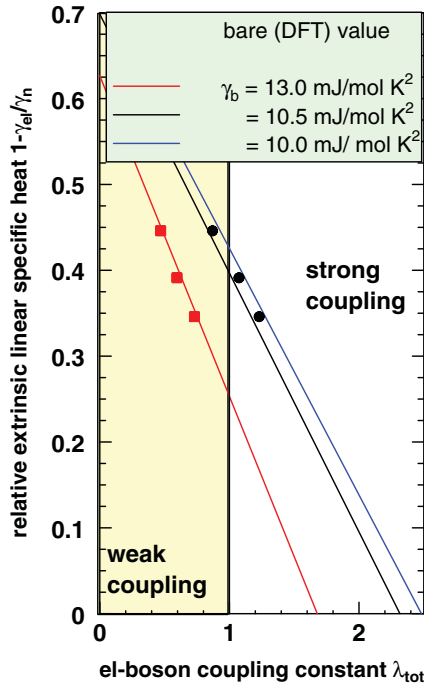
FIG. 3. (Color online) The relative extrinsic linear specific heat coefficient of KFe$_2$As$_2$ using the experimentally observed nominal $\gamma_n = 94$ mJ/mol K$^2$ vs. the total electron-boson coupling constant $\lambda_{tot}$ given by Eqs. (4) and (7) for various bare $\gamma_b$ values obtained from density of states as calculated by various DFT codes[22,25,26] (see text) and using a typical high-energy renormalization factor of $\eta = 2.7$ [see Eq. (4)]. The data points show the results of simulations within single band $d$-wave Eliashberg theory to reproduce $T_c = 3.5$ K and a spectral density for spin fluctuations adopted from recent Institute for Nuclear Studies data[7] and including also a weak electron-phonon interaction and a weak Coulomb pseudopotential $\mu^*$ (details are discussed in the text).

strong-coupling scenario can be excluded from this point of view. There are at least two experimental hints that clearly point to the existence of an extrinsic subsystem that manifests itself in a substantial residual linear specific heat visible at very low $T$ at ambient fields (see Fig. 8) and in high fields of about 9 T where the superconductivity is well suppressed (see inset of Fig. 2). From the latter one estimates $\gamma_{el} \leqslant 70$ mJ/mol K$^2$. In the next section, we will provide theoretical arguments in favor of a significantly reduced intrinsic Sommerfeld term $\gamma_{el}$.

### C. Theoretical estimates of the thermal mass enhancement

#### 1. Kadowaki-Woods analysis

The weak-coupling result can be understood at a qualitative level also by analyzing the so-called Kadowaki-Woods relation (KWR), $\kappa_{KWR} = A_\rho/\gamma_v^2$, where $A_\rho$ describes the $T^2$ contribution to the resistivity at very low $T$: $\rho(T) = \rho_0 + A_\rho T^2$ observed so far only in a few very clean samples[25] with an extremely large residual resitivity ratio $\rho(300\ \text{K})/\rho(5\ \text{K}) \approx 500$ and where $\gamma_v$ is the volumetric Sommerfeld coefficient. The latter is related to the usually used molar quantity $\gamma_0$ in the present case (with two KFe$_2$As$_2$ units per unit cell) by
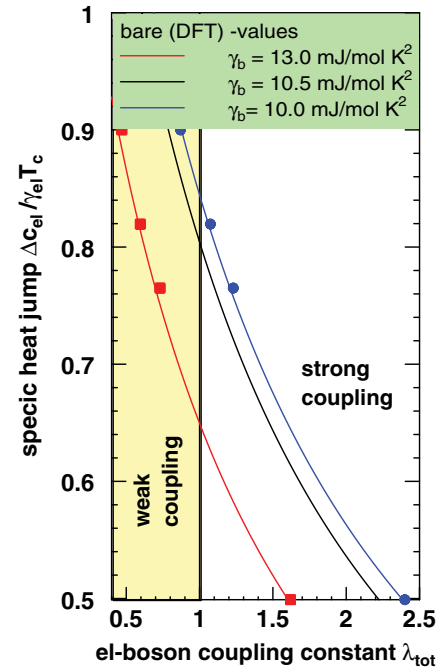


FIG. 4. (Color online) The normalized specific heat jump at $T_c$ vs. the phenomenological total electron-boson coupling constant $\lambda$ and various DFT-derived bare linear specific heat values.[22,25,26] (Red and blue symbols) Results using the corresponding $\gamma_{el}$ values from Fig. 3 extended by two strong-coupling points for $\gamma_{el} = \gamma_n$ and the experimental value of $\Delta c_{el}/T_c = 45.6$ mJ/mole K$^3$.

the relation

$$\gamma_v = 2\gamma_0/N_A V_u,$$

where $N_A$ denotes Avogadro's number and $V_u = 204.2$ Å$^3$ is the unit cell volume of KFe$_2$As$_2$. Then, following Hussey,[30] one has for the case of a (quasi)-2D system with cylindrical Fermi surface sheets,

$$\kappa_{KWH} = \frac{A_\rho}{\gamma_v^2} = \frac{72\pi\hbar}{e^2 k_B^2} \frac{ac_*^3}{k_{F,el}^3} = \propto n_{el}^{-1.5}, \quad (2)$$

where $a = 3.8414$ Å is a tetragonal lattice constant and $c_* = 0.5c = 6.9185$ Å, i.e., half of the lattice constant along the stack direction. Notice the *cancellation* of many-body renormalizations on the right-hand side but the somewhat different exponent, $-1.5$, for the electron density $n_{el}$ as compared with $\propto n_{el}^{-2}$ within a similar expression proposed recently and given here for comparison also for the 2D case:[31]

$$\kappa_{KWJ} = \frac{A_\rho}{\gamma_{0,el}^2} = \frac{81\pi\hbar}{4k_B^2 e^2 n_{el}^2} \propto n_{el}^{-2}. \quad (3)$$

Since in the stoichiometric case of K-122 there is exactly one hole in the three bands (i.e., per formulas unit) which cross the Fermi energy, one obtains for the corresponding electron density $n_{el} = 4.9 \times 10^{28}$ m$^{-3}$ and

$$k_{F,el} = \sqrt{2\pi n_{el} c_*} = 1.46 \times \text{Å}^{-1}$$

for the 2D-effective Fermi wave vector of electrons. Inserting our value of $k_{F,el}$ into Eq. (2), one arrives at $\gamma_v =$

0.67 mJ/K$^2$ cm$^3$ or $\gamma_{0,\text{el}} \approx 69$ mJ/mol K$^2$ $< \gamma_n$. Using instead Eq. (3), one obtains a slightly smaller value $\gamma_{0,\text{el}} \approx 37$ mJ/mol K$^2$ that, again, is significantly smaller than our nominal value $\gamma_n \approx 94$ mJ/mol K$^2$. [In both Eqs. (2) and (3) the experimental value $A_\rho = 3 \times 10^{-2}$ $\mu\Omega$cm has been used as reported in Ref. 25.] Thus, our empirical value of about 60 mJ/mol K$^2$[20] can be regarded as a reasonable number. In view of the idealized electronic structure in terms of the cylindric Fermi surface sheet (FSS) adopted above, a more realistic and sophisticated multiband analysis is desirable. To illustrate this point we consider the simple case when all four FSS would give the same contribution to the resistivity and to the specific heat. Applying the Kadowaki-Woods relation, first, to such a hypothetical single FSS, we would arrive, finally, at $\gamma_n \approx 74$ mJ/mol K$^2$ in the case of Eq. (3). Since different individual residual resistivities $\rho_i, i = 1$–4, lower these values, we regard these two numbers as upper and lower bounds for a more realistic $\gamma_{0\text{el}}$ somewhere in between. More theoretical microscopic studies, including the determination of the individual residual resistivities, are necessary to improve the accuracy of these Kadowaki-Woods-type relations for pronounced multiband systems. Note that our empirical value of about 60 is very close to the mean value, $0.5(37 + 74) \approx 56$. (A more detailed consideration will be given in future work.) By considering also available data for the in-plane penetration depth (or the condensate density) in the superconducting state at very low $T$, one arrives at similar estimates (see below). Considering this, we strongly believe that the nominal value of about 94 mJ/mol K$^2$ given above, and similar numbers found in the recent literature,[21] significantly *overestimate* the contribution from the itinerant electrons that bear the superconductivity.

The nominal value of $\gamma_n$ should be compared with the calculated quantity of $\gamma_b = 10.2$ to 13.0 mJ/mol K$^2$ from DFT-based band structure calculations,[22,25,26] which can be regarded as the unrenormalized bare quantity. The renormalization happens in two steps at different energy scales: a first one at high energies which is governed by the Coulomb interaction and/or Hund's rule coupling and a second on at low energies which is governed by the interaction of the quasiparticles with various bosonic excitations (phonons, paramagnons, magnons, etc.). The high-energy renormalization yields for typical transition metals a mass enhancement by a factor of 2 to 3 as evidenced by a general band squeezing as observed, for instance, in ARPES measurements[5,6] or in optics measurements comparing calculated and measured unscreened plasma frequencies. For example, taking a typical 122 experimental in-plane plasma frequency of 1.55 eV[28] to be compared with the calculated DFT value of 2.56 to 2.58 eV[25,26] yields a considerable mass enhancement of $\eta \approx 2.7$, in accordance with the high-energy band "squeezing" factor of about 2 to 3 as seen by ARPES.[5,6] Thus, one is left with an effective quasiparticle (qp) $\gamma_{\text{qp}}$ quantity of about 30 to 40 mJ/mol K$^2$ to be compared with our empirical estimate of about 60 mJ/mol K$^2$. This value is further modified by coupling to bosons, such as phonons and spin fluctuations, and one writes,

$$\gamma_{\text{el}} = \gamma_{\text{qp}}[1 + \lambda_{\text{ph}} + \lambda_{\text{sf}}], \quad \gamma_{\text{qp}} = \eta\gamma_b, \quad \eta \approx \Omega^2_{\text{pl,DFT}}/\Omega^2_{\text{pl,opt}},$$

(4)

where $\lambda_{\text{ph}}$ is the electron-phonon coupling constant, $\lambda_{\text{sf}}$ is the enhancement due to spin fluctuations (antiferromagnetic paramagnons), and $\eta > 1$ denotes the high-energy renormalization. In the case of Fe-based superconductors, the conventional electron-phonon interaction is weak, yielding $\lambda_{\text{ph}} \lesssim 0.2$,[32] which is insufficient to explain the large $\gamma_{\text{el}}$ value obtained from specific heat measurements. A similar value has been found also for KFe$_2$As$_2$: $\lambda_{\text{ph}} \approx 0.17$ (details of this DFT based calculation will be given elsewhere). Taking this into account, we may finally estimate that $\lambda_{\text{sf}} \lesssim 1$ in the case of KFe$_2$As$_2$.

### 2. Penetration depth and condensate density

The conclusion about weak electron-boson coupling is also supported using the experimental value of the in-plane penetration depth extrapolated to $T = 0$: $\lambda_{\text{ab},L} \approx 203$ nm (measured at 50 mK)[33] and $\lambda_{\text{ab},L} \approx 194$ nm (measured at 20 mK).[34] Following Refs. 27, 35, and 36 one has for the *renormalized* plasma frequency that enters the penetration depth (rewritten in convenient units)

$$\Omega_{\text{pl}}(\text{eV})\lambda_L(\text{nm}) = 197.3\sqrt{DNZ_m}, \quad DNZ_m > 1,$$

(5)

where $N = n_{\text{tot}}/n_s$ is the reciprocal number of the conduction electron density involved in the superconducting condensate, $Z_m \approx [1 + \lambda_{\text{tot}}(0)]$ describes the dynamical mass renormalization, and $D = (1 + \delta)(1 + f)$ with $\delta, f > 1$ describes the effect of disorder and fluctuations of competing phases. In the clean limit one has $\delta \to 0$. For the sake of simplicity we will ignore the influence of fluctuations. Using $\hbar\Omega_{\text{pl}} = 1.55$ eV for the expected unscreened experimental plasma frequency (i.e., the experimental high-$T$ plasma energy with no or small renormalizations due to the electron-boson couplings), one has

$$(2.33 \text{ to } 2.64)\frac{n_s}{n_{\text{tot}}} = (1 + \lambda_{\text{ph}} + \lambda_{\text{sf}})(1 + \delta),$$

(6)

where $\delta \sim 1/4$ to $1/3$ measures the remaining weak disorder and the reciprocal gap amplitude related parameter close to that in the clean limit (i.e., $\delta \ll 1$). Furthermore, for the sake of simplicity, we will assume that all electrons are involved in the superconducting condensate, i.e., $N \equiv 1$ (just for illustration see also the special case $n_s/n \approx 0.74$ mentioned in our remark).[37] One then arrives at the following constraint:[38]

$$\lambda_{\text{tot}} = \lambda_{\text{ph}} + \lambda_{\text{sf}} \approx 0.87 \text{ to } 0.97 \quad \text{or} \quad \lambda_{\text{sf}} \approx 0.7 \text{ to } 0.8,$$

(7)

in accord with a close estimate from $\gamma_{\text{el}} \sim 60$ mJ/mol K$^2$, our calculated $\lambda_{\text{ph}} = 0.17$, and $\gamma_b \approx 10.5$ mJ/K$^2$ mol from DFT calculations[26] and Eq. (4).
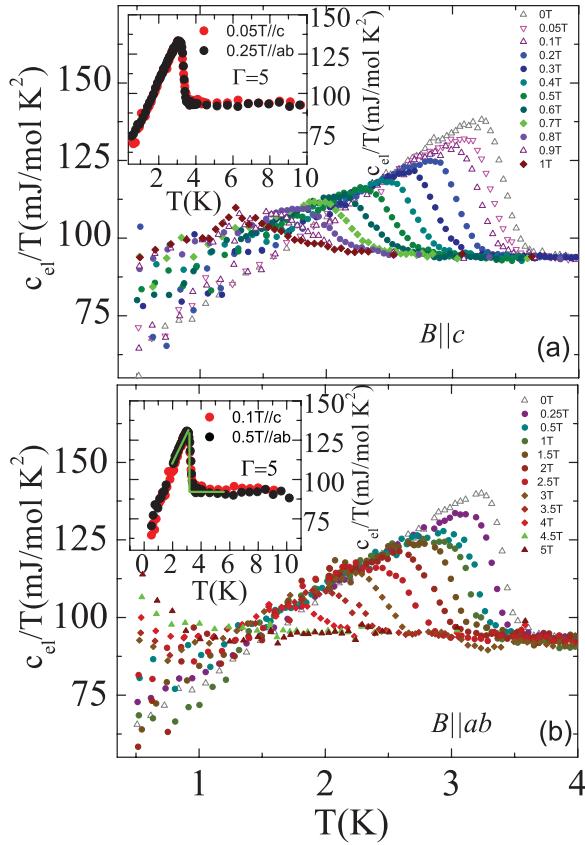
FIG. 5. (Color online) The electronic specific heat coefficient $c_{el}/T$ of KFe$_2$As$_2$ (after subtracting the phonon contribution) for both directions $B \parallel c$ and $B \parallel ab$ as shown in (a) and (b), respectively. In order to determine the $T_c$ of KFe$_2$As$_2$, an entropy-conserving construction was used as shown with a green line in the inset of (b). The insets of the upper and lower panels show two data sets with the same $T_c$ value for the two directions, confirming our anisotropy ratio, $\Gamma \sim 5$.

### D. The upper critical fields $H_{c2}(T)$ and their anisotropy

Figures 5–7 summarize the $T$ dependence of the specific heat data $c_p$ for the investigated KFe$_2$As$_2$ single crystal in various magnetic fields applied parallel and perpendicular to the $ab$ plane. With increasing applied magnetic field in both directions, the superconducting anomaly shifts and broadens systematically to lower $T$ and is also reduced in height. In an applied magnetic field of 9 T, superconductivity is completely suppressed for both directions of our crystal. In order to analyze the phase diagram of the field dependence of $T_c$, we used an entropy-conserving construction of the electronic specific heat to determine $T_c$ of both orientations as shown in Fig. 5. Then, in a very first step, the upper critical field and its slope near $T_c$ can be estimated by the Ginzburg-Landau (GL) equation[39,40] (strictly speaking valid near $T_c$, only),

$$H_{c2} = H_{c2}(0)\left[\frac{1-t^2}{1+t^2}\right], \quad (8)$$

where $t = T/T_c$. The upper critical field values at $T = 0$ have been evaluated to $\mu_0 H_{c2}^{(c)}(0) = 1.8$ T and $\mu_0 H_{c2}^{(ab)}(0) = 8.6$ T and the fits are shown via dashed black lines in Fig. 6. In the case of $H_{c2}$ obtained from ac susceptibility data (see above
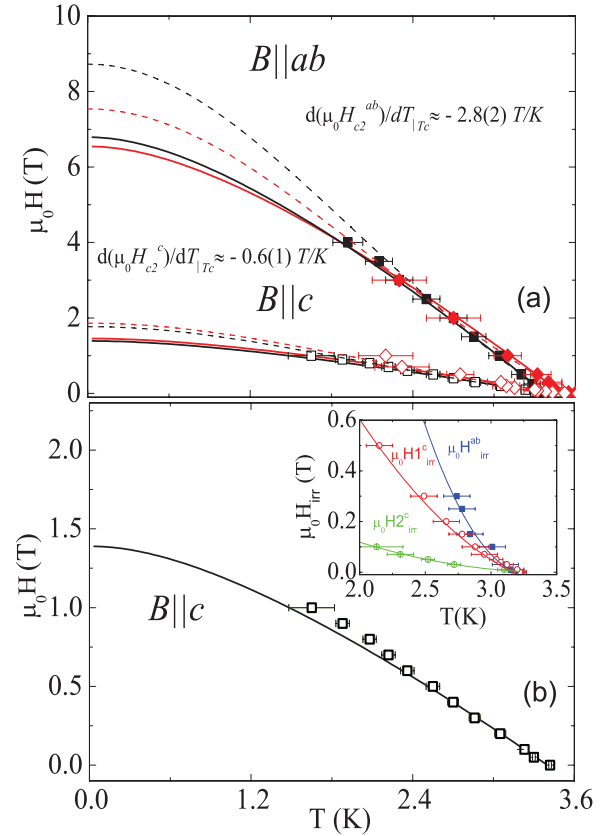


FIG. 6. (Color online) Phase diagram of $\mu_0 H_{c2}(T)$ for KFe$_2$As$_2$ with the magnetic field applied parallel and perpendicular to the $c$ axis from specific heat (black symbols) and ac susceptibility measurements (red symbols). (Solid lines) Theoretical curves based on the WHH model ($\alpha = 0$). (Dashed curves) GL theory. (Inset) $T$ dependence of $H_{irr}$ obtained from ac susceptibility measurements as discussed in the text.

Fig. 1), we arrive at slightly different values of $\mu_0 H_{c2}^{(c)}(0) \approx 1.9$ T and $\mu_0 H_{c2}^{(ab)}(0) \approx 7.5$ T, respectively (dashed red curves).

It is interesting to compare the obtained and extrapolated to $T = 0$ anisotropy ratio for the upper critical field of about 4.5 with that ratio for the penetration depth[34] (i.e., $\lambda_{L,ab} = 194.3$ nm and $\lambda_{L,c} = 510.3$ nm taken at $T = 20$ mK) that yields 2.63 for a sample with $T_c \approx 3.14$ K only. (A somewhat larger anisotropy ratio, $\sim 4$, has been announced based on preliminary small-angle neutron-scattering data[41] for a crystal with a higher $T_c \approx 3.6$–4.1 K ) For a simple one-band model or separable multiband models,[12] including a phenomenological mass anistropy, one would expect

$$\Gamma_0 \approx \left(\frac{m_c}{m_{ab}}\right)^{1/2} = \frac{\lambda_{L,c}(0)}{\lambda_{L,ab}(0)} = \frac{H_{c2\parallel ab}(0)}{H_{c2\parallel c}(0)} \approx 4.5. \quad (9)$$

From full relativistic DFT calculations an out-of-plane plasma frequency of 0.61 eV has been obtained,[26] which suggests a mass anisotropy of 4.38 slightly exceeding the value of 3.27 for Ba-122.[42] Thus, the observed anisotropy derived from the upper critical fields exceeds this value, whereas the penetration depth gives a slightly smaller value. We ascribe this small deviation of our empirical $\Gamma_0$ from the simple mass anisotropy to (i) the anisotropy of the pairing interaction and,
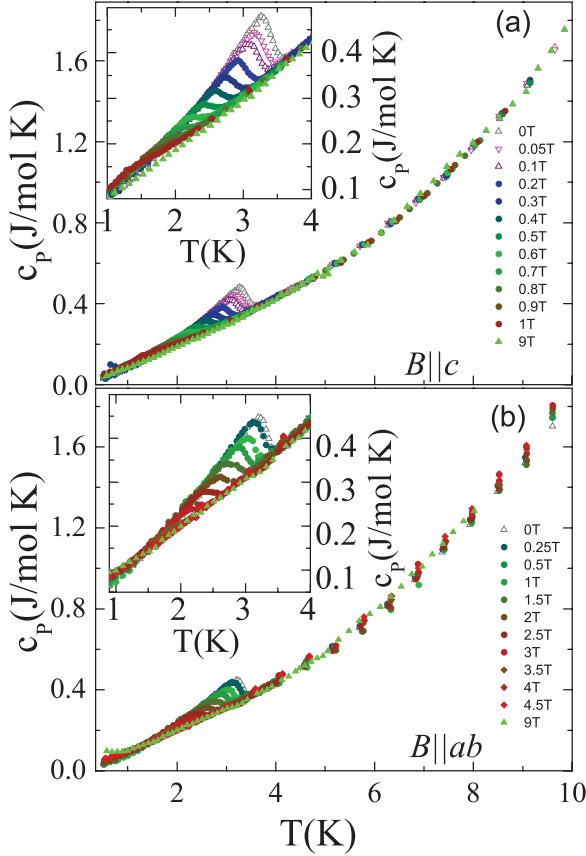
FIG. 7. (Color online) The $T$ dependence of the specific heat of $KFe_2As_2$ in various applied magnetic fields up to 9 T parallel to the $c$ axis (a) and parallel to the $ab$ plane (b). The insets of the upper and lower panels show a close-up of the superconducting state for both directions.

consequently, also of the order parameter[34] and/or oppositely of the depairing interaction that all might additionally enhance $H_{c2\|ab}$ and suppress $\lambda_{L,ab}$ or, vice versa, the corresponding $c$ components. For instance, the anisotropic screening and significantly anisotropic plasma frequencies might cause an anisotropic Coulomb pseudopotential $\mu^*$. In case of a magnetic spin fluctuation-based mechanism, the in-plane anisotropy observed for ordered magnetic structures should act in a similar way.

(ii) One should also take into account that, strictly speaking, the upper critical fields and the penetration depth at $T = 0$ probe various subgroups of electrons with different Fermi-velocity-dependent weights, whereby the penetration depth probes more sensitively fast electrons $\lambda_{L,i}^{-2} \propto \Omega_{pl,i}^2$, where $\Omega_{pl,i}$ denotes the corresponding $i^{th}$ subgroup plasma frequency and the total penetration depth is given by $\lambda_L^{-2} = \sum_i \lambda_{L,i}^{-2}$. In contrast, the upper critical fields are more sensitive to slow electrons since $H_{c2\|ab} \propto (\Phi_0/v_x v_z)$, where $\Phi_0$ denotes the flux quantum. Finally, (iii) anisotropic impurity scattering rates might also affect $\Gamma_0$.

Another possibility to estimate roughly the upper critical field $H_{c2}(0)$ is to consider the single-band Werthamer-Helfand-Hohenberg (WHH) formula[43] with the Maki parameter $\alpha = 0$. As shown with solid lines in Fig. 6, the specific heat and ac

magnetization $H_{c2}$ data for $B \parallel ab$ are perfectly described by the WHH model with an average slope of $-d(\mu_0 H_{c2}^{(ab)})/dT \approx 2.8(2)$ T/K while for $H \parallel c$ the single-band WHH model with $-d(\mu_0 H_{c2}^{(c)})/dT = 0.55(5)$ T/K underestimates the specific heat data (see the lower panel of Fig. 6). From these values the upper critical fields $\mu_0 H_{c2}(0)$ are found to be ~1.4 T and ~7 T for the $c$ and $ab$ direction, respectively. The observed small difference between $H_{c2}$ obtained from the specific heat and the ac magnetization data is not surprising since these methods naturally imply different criteria for $T_c$ determination.

In the case of a multiband superconductor, the low-$T$ $H_{c2}$ curve may exceed the single-band WHH predictions.[45] Therefore, we suppose that the observed deviation from the single-band WHH model is related to multiband effects. Additionally, indications of a two-band-like behavior of our single crystal was observed in zero-field specific heat measurements (as we will discuss below). Neglecting these effects and using typical slow renormalized Fermi velocities $v_F \sim 5 \times 10^4$ m/s derived from preliminary ARPES data[6] and $T_c = 3.5$ K, one estimates also, in principle, within a two-band approach adopting $s$ symmetry,[46,47] a slope value of

$$H'_{c2,c} = -\frac{24\pi k_B^2 T_c \Phi_0}{7\zeta(3)\hbar^2 \left(c_1 v_1^2 + c_2 v_2^2\right)}, \qquad (10)$$

where $c_1 \rightarrow c_2 \rightarrow 1/2$ and $v_F \sim \sqrt{(2)}v_1, \sqrt{(2)}v_2$ in the case of a dominant interband pairing and $\zeta(3) \approx 1.202$, resulting in $-dH_{c2}^c/dT = \sim 0.5$ T/K near $T_c$, which is already very close to our experimentally determined value and is also in accord with the renormalized Fermi velocity of $4 \times 10^6$ cm/s using the total bare velocity $1.77 \times 10^7$ cm/s from the full relativistic (not spin-polarized) LDA calculations and the FSS averaged renormalizations contained in the intrinsic $\gamma_{el}$ value of about 60 mJ/K$^2$ mol estimated above. In comparison, the reported values determined via detailed resistivity studies on $KFe_2As_2$ single crystals yield lower values, i.e., $H_{c2}^c = 1.25$ T and $H_{c2}^{ab} = 4.47$ T, where a low value of $T_c = 2.8$ K has been reported.[4] The anisotropy of the slopes near $T_c$ *as measured* of about 5.35 is very close to the value found here: 5.09. The reported larger value of 6.8 seems to be a consequence of the extremely high anisotropic spin-orbit coupling $\lambda_{so} = 0.36$ for $B \parallel ab$ and $\infty$ for $B \parallel c$ adopted in Ref. 4 in analyzing their data.[48] The reported *larger* absolute slope values might be interpreted as a hint for an impurity driven transition to an $s$-wave superconductor with $\langle\Delta\rangle_{FS} \neq 0$ with pair breaking [see Eq. (A3) in Ref. 12]. From our studies, further information about the anisotropy of $KFe_2As_2$ single crystals can be obtained, which is $\Gamma_{T \rightarrow T_c} = H_{c2}^{ab}/H_{c2}^2 \sim 5$ (see also the insets of Fig. 5). Surprisingly, this anisotropy value is comparable with $\Gamma_{T \rightarrow T_c}$ values of, e.g., $NdFeAsO_{0.82}F_{0.18}$[49] and LaFePO[50] showing a more anisotropic electronic structure (9.2 to 10.8 for LaFeAsO and 4.16 to 5.04 for LaFePO) and might be, therefore, ascribed to opposite anisotropies of the order parameter. On the other hand, it is considerably larger than the typical values of $\Gamma_{T \rightarrow T_c} \sim 2$ and 2.6 found for nearly optimally hole-doped $BaKFe_2As_2$[51,52] but lower than the ones determined for $SmFeAsO_{0.85}F_{0.15}$ and La(O,F)FeAs thin films.[10,53]

The $T$ dependence of the irreversibility field $H_{irr}$ obtained from $\chi''_v$ are shown in the inset of Fig. 6 (see above). The low

value of $H_{irr}^{ab}$ for $B \parallel ab$ is related with a large anisotropy and a weak pining, as expected in the case of clean single crystals. We attribute the $H1_{irr}^{c}$ with a peak effect in the $T$ dependence of the critical current $J_c$ for $H \parallel c$ in accord with similar observations on YBCO single crystals[18] that exhibit a rather similar anisotropy of the upper critical field and, therefore, a similar pinning behavior also can be expected.

### E. Aspects of the electronic specific heat in the superconducting state: The residual linear specific heat and the jump at $T_c$

The height of the specific heat jump $\Delta c_{el}/T_c \approx 45.6$ mJ/mol K$^2$ at $T_c$ is found from our zero-field electronic specific heat data. This value exceeds the value that has been reported for a polycrystalline KFe$_2$As$_2$ sample[2] but is a factor of 2 lower than the one obtained for the nearly optimally hole-doped Ba$_{0.6}$K$_{0.4}$Fe$_2$As$_2$.[51] For our estimated $\gamma_{el} \sim 60$ mJ/mol K$^2$, the ratio $\Delta c_{el}/\gamma_{el}T_c$ was found to be enhanced as compared with the use of the nominal value, near about 0.76 versus 0.49 (see Fig. 4), and still significantly lower than the result of the Bardeen-Cooper-Schrieffer (BCS) weak-coupling approximation, $\Delta c_{el}/\gamma_{el}T_c = 1.43$.[54] This points toward a multiband (gap) scenario with $s$-, $p$-, or $d$-wave pairing. In particular, this value is close to the value reported for the $p$-wave superconductor SrRuO$_4$ with $\Delta c_{el}/\gamma_{el}T_c = 0.73$.[55]

In a clean situation with negligible pair-breaking effects, the reduced jump in the specific heat $\Delta c_{el}/T_c\gamma_{el}$ compared to that of a single-band $s$-wave superconductor might be related to unconventional superconductivity with nodes as discussed above and/or a pronounced multiband character with rather different partial densities of states and gap values. Futhermore, in relatively dirty systems, unconventional superconductivity might be driven into an $s$-wave state. To illustrate the multiband character, we adopt here, for the sake of simplicity, a simple effective weak-coupling $s$-wave model like in Ref. 24. Another interesting issue we would like to address concerns what happens with the "extrinsic" linear specific heat at very low $T$. Thus, fitting the electronic part of the specific heat within a two-band model (see the blue curves in Fig. 8) while admitting also a "residual" linear Sommerfeld part, we arrive at a relatively large value of $\gamma_{res}(T \rightarrow 0) \approx 15$ mJ/mol K$^2$ that might be related to an "extrinsic" pair-breaking contribution that is somewhat suppressed deep in the superconducting state.[37] We admit that the adopted $s$-wave analysis might provide only an upper limit, since, for an unconventional pairing symmetry, the spectral weight at low $T$ is enhanced. Moreover, the final density of states introduced by pair-breaking-induced subgap states might also contribute to this value. Thus, more sophisticated multiband models, including interacting pair-breaking impurity states, are likely necessary to settle this interesting problem. Due to its complexity, such a treatment is, however, beyond the scope of the present paper. Specific heat measurements below 0.2 K would also be helpful in order to further refine the value of $\gamma_{res}$. In this context, the observation of substantial residual terms in other pnictide or chalcogenide superconductors is noteworthy. For instance, in the systems FeTe$_{0.57}$Se$_{0.45}$ and Co-doped Ba-122, a relatively large (8% and 25%, respectively) residual linear contribution has been observed.[56,57]
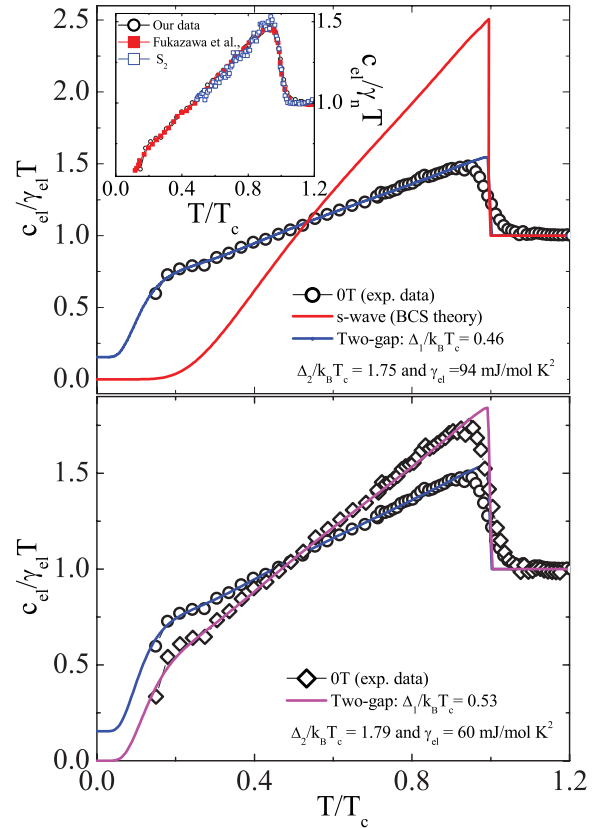


FIG. 8. (Color online) (Upper panel) Fit under the assumption of no extrinsic contribution to the linear specific heat (see also Figs. 3 and 4). The normalized superconducting electronic specific heat $c_{el}/(\gamma_{el}T)$ of KFe$_2$As$_2$ as a function of the reduced temperature $t = T/T_c$. The red line represents the theoretical curve for the single-band weak-coupling BCS case ($\Delta_0/k_BT_c = 1.76$). The blue line shows the curve of the nodeless weakly coupled two-gap model fit; for details see the text. The inset shows our electronic specific heat data in comparison with data by Fukazawa *et al.*,[21] together with an another sample that shows that our $T_c$ is similar to that of the investigated sample. (Lower panel) Fit assuming that a significant contribution to the linear specific heat is not intrinsic using, e.g., $\gamma_{el} = 60$ mJ/mol K$^2$ taken from Ref. 20 (see Figs. 3 and 4).

Finally, for completeness, we discuss the various gap values obtained in the present simple model for analyzing the $T$ dependence of our zero-field specific heat measurements down to 400 mK. The normalized zero-field electronic specific heat $c_{el}/\gamma_n T$ is shown in Fig. 8. First, we compare our data to the single-gap BCS theory (i.e., a weak-coupling approach using $\Delta_0/k_BT_c = 1.76$ at $T_c$) and find that a single BCS gap cannot be reconciled with our experimental data.

Since a single-gap scenario cannot describe our data, we applied a phenomenological two-gap model in line with multigap superconductivity reported by various experimental and theoretical studies on different compounds within the FeAs family.[2,58–60] We have analyzed our data utilizing the generalized $\alpha$ model, which has been proposed to account for the thermodynamic properties of multiband, multigap superconductors like, e.g., MgB$_2$.[61] In this approach the

one-band expression

$$\frac{S}{\gamma_{el}T_c} = -\frac{6\Delta_0}{\pi^2 k_B T_c} \int_0^\infty [f \ln f + (1-f)\ln(1-f)]dy, \tag{11}$$

$$\frac{c_{el}}{\gamma_{el}T_c} = t \frac{d\left(\frac{c_{el}}{\gamma_{el}T_c}\right)}{dt}, \tag{12}$$

is straightforwardly generalized to the two-band case and entropy conservation is adopted for each band. In Eq. (11) the Fermi function is denoted by $f = 1/[\exp(\beta E) + 1]$, $\beta = (k_B T)^{-1}$, and the energy of the quasiparticles is given by $E = [\epsilon^2 + \Delta^2(t)]^{0.5}$, with $\epsilon$ being the energy of the normal-state electrons measured relative to the Fermi surface. The integration variable is $y = \epsilon/\Delta_0$. Finally, (S) and (C) are the thermodynamic properties, and $t = T/T_c$ is the reduced temperature. In Eq. (11) the scaled gap $\alpha = \Delta_0/k_B T_c$ is the only adjustable fitting parameter for a single-band case. The temperature dependence of the gap is determined by $\Delta(t) = \Delta_0 \delta(t)$, where $\delta(t)$ is approximately described by the data taken from the table in Ref. 62. In the case of a two-band model, the thermodynamic properties are obtained as the sum of the contributions from the individual bands, i.e., $\alpha_1 = \Delta_1(0)/k_B T_c$ and $\alpha_2 = \Delta_2(0)/k_B T_c$ with their respective weights $\gamma_1/\gamma_m$ and $\gamma_2/\gamma_{el}$.

To calculate the theoretical curves $c_{el}/\gamma_{el}T$, the parameters $\Delta_1$, $\Delta_2$, their respective ratios $\gamma_1$ and $\gamma_2$, and the ratio $\gamma_{res}/\gamma_{el}$ are left for free as an additional, third, fitting parameter ($\gamma_{res}$ represents the non-negligible residual value at low $T$). The best description of the experimental data is obtained using values of $\Delta_1/k_B T_c = 0.46$ and $\Delta_2/k_B T_c = 1.75$. The calculated specific heat data are represented by the solid blue line in Fig. 8 (upper panel). Small relative jumps are not compatible with the strong-coupling scenario estimated in Fig. 4 for the case of no extrinsic contributions. Therefore, we performed a second analysis where the effective extrinsic linear contibution necessary for a weak-coupling scenario has been subtracted from the raw data. The result is shown in the lower panel of Fig. 8. In this case, both gaps slightly increase to 1.8 K and 6.2 K.

The obtained gap values are comparable with the two-band $s$-wave fit for the penetration depth data of K-122[34] (H ∥ $c$: 1.28 K and 5.31 K) and do not clearly exceed the corresponding values for the isomorphic compound $RbFe_2As_2$ with a lower $T_c$ value of 2.52 K only: 1.74 K and 5.7 K.[60] In our opinion, that similarity might reflect the presence of nodes in the superconducting order parameter of $KFe_2As_2$. A detailed comparison of these two closely related systems would be very interesting, especially, if, in fact, it would be confirmed that the symmetry of the order parameter would differ.

Although a clear picture is still missing for the case of $KFe_2As_2$, it is important to emphasize that our system definitely underlies multiband superconductivity, probably in the weak-coupling regime. However, from specific heat data alone it is difficult to be sure whether nodes exist, since in the case of multiband superconductivity low-energy quasiparticle excitations can be always explained by the contribution from an electron group with a small gap. We believe that further experimental studies such as specific heat well below 400 mK, ARPES, and transport investigations at very low $T$ will

be helpful to elucidate the nature of superconductivity in $KFe_2As_2$.

## IV. CONCLUSIONS

In summary, $KFe_2As_2$ was investigated by ac susceptibility and low-$T$ specific heat measurements on high-quality single crystals grown by a self-flux technique. The specific heat jump was found to be $\Delta c_{el}/T_c \sim 45.9$ mJ/mol K$^2$ and the nominal Sommerfeld coefficient $\gamma_n = 94(3)$ mJ/mol K$^2$. However, several theoretical considerations, including two recently proposed modified Kadowaki-Woods relations, as well as the observation of a significant linear in $T$ residual term, point to a significantly *smaller* value of about 60 mJ/mol K$^2$ for the Sommerfeld coefficient for the itinerant quasiparticles. This suggests that the strongly correlated "heavy-fermion-like" scenario suggested for K-122 in the literature should be revisited. In this context the elucidation of the "external" subsystem responsible for that difference is a challenging problem to be considered in future work. In terms of bosonic mode coupling, the total electron-boson coupling constant $\lambda_{tot} = \lambda_{ph} + \lambda_{sf} \sim 1$ avaraged over all Fermi surfaces inferred here excludes strong coupling while the calculated weak electron-phonon coupling of about 0.17 points to a dominant spin-fluctuation mechanism and unconventional superconductivity.

The magnetic phase diagram has been studied yielding values for the upper critical fields $\mu_0 H_{c2}^c(0) \approx 1.4$ T and $\mu_0 H_{c2}^{ab}(0) \approx 7$ T for the $c$ axis and $ab$ plane, respectively. The resulting anisotropy of $KFe_2As_2$ near $T_c$ lies around $\Gamma_{T \to T_c} = H_{c2}^{(ab)}/H_{c2}^{(c)} \sim 5$, which slightly exceeds the mass anisotropy as derived from DFT-electronic structure calculations, as well as the anisotropy of the penetration depth. But at $T = 0$ all these anisotropies become rather close, tending to be about 4.5, including also preliminary penetration depth data of Ref. 41.

For a full understanding of the gap structure of $KFe_2As_2$, as well as of the high values of $c_{el}/\gamma_{el}T$ at low temperatures, further specific heat measurements at very low $T < 400$ mK like in Ref. 14 but analyzed quantitatively with respect to various magnetic and superconducting contributions and/or low-$T$ ARPES and transport studies will be helpful. Finally, the irreversibility field $H_{irr}$ derived from ac susceptibility data has been investigated. The double maximum in $\chi''_v(T)$ for $H \| c$ suggests the presence of a peak effect in the $T$ dependence of the critical current.

*m.mohamed@ifw-dresden.de

[1] Y. Kamihara, T. Watanabe, M. Hirano, and H. Hosono, J. Am. Chem. Soc. **130**, 3296 (2008).

[2] H. Fukazawa, Y. Yamada, K. Kondo, Y. Kohori, K. Kuga, Y. Matsumoto, S. Nakatsuji, H. Kito, P. M. Shirage, K. Kihou *et al.*, J. Phys. Soc. Jpn. **78**, 083712 (2009).

[3] K. Kihou, T. Saito, S. Ishida, M. Nakajima, Y. Tomioka, H. Fukazawa, Y. Kohori, T. Ito, S. Uchida, A. Iyo *et al.*, J. Phys. Soc. Jpn. **79**, 124713 (2010).

[4] T. Terashima, M. Kimata, H. Satsukawa, A. Harada, K. Hazama, S. Uji, H. Harima, G.-F. Chen, J.-L. Luo, and N.-L. Wang, J. Phys. Soc. Jpn. **78**, 063702 (2009).

[5] T. Sato, K. Nakayama, Y. Sekiba, P. Richard, Y.-M. Xu, S. Souma, T. Takahashi, G. F. Chen, J. L. Luo, N. L. Wang, and H. Ding, Phys. Rev. Lett. **103**, 047002 (2009).

[6] D. V. Evtushinsky (private communication).

[7] C. H. Lee, K. Kihou, H. Kawano-Furukawa, T. Saito, A. Iyo, H. Eisaki, H. Fukazawa, Y. Kohori, K. Suzuki, H. Usui, K. Kuroki, and K. Yamada, Phys. Rev. Lett. **106**, 067003 (2011).

[8] T. Terashima, M. Kimata, N. Kurita, H. Satsukawa, A. Harada, K. Hazama, M. Imai, A. Sato, K. Kihou, C.-H. Lee *et al.*, J. Phys. Soc. Jpn. **79**, 053702 (2010).

[9] M. Kimata, T. Terashima, N. Karita, H. Satsukawa, A. Harada, K. Kadoma, K. Takehana, Y. Imanaka, T. Takamasu, K. Kihou *et al.*, Phys. Rev. Lett. **107**, 166402 (2011).

[10] U. Welp, C. Chaparro, A. E. Koshelev, W. K. Kwok, A. Rydh, N. D. Zhigadlo, J. Karpinski, and S. Weyeneth, Phys. Rev. B **83**, 100513(R) (2011).

[11] J. L. Zhang, L. Liao, Y. Chen, and H. Q. Yuan, Front. Phys. **6**(4), 463 (2011).

[12] V. G. Kogan, Phys. Rev. B **80**, 214532 (2009).

[13] Kim *et al.*[14] have also studied the magnetic phase diagram of KFe$_2$As$_2$ by specific heat measurements. However, in their studies they used a batch of several single crystals glued on top of each other, which is less favorable than using only one piece of a single crystalline material.

[14] J. S. Kim, E. G. Kim, G. R. Stewart, X. H. Chen, and X. F. Wang, Phys. Rev. B **83**, 172502 (2011).

[15] M. I. Tsindlekht, I. Felner, M. Zhang, A. F. Wang, and X. H. Chen, Phys. Rev. B **84**, 052503 (2011).

[16] J. A. Osborn, Phys. Rev. **67**, 351 (1945).

[17] F. Gömöry, Supercond. Sci. Technol. **10**, 523 (1997).

[18] J. Giapintzakis, R. L. Neiman, D. M. Ginsberg, and M. A. Kirk, Phys. Rev. B **50**, 16001 (1994).

[19] E. S. Vlakhov, K. Nenkov, M. Ciszek, A. Zaleski, and Y. Dimitriev, Physica C **225**, 149 (1994).

[20] V. A. Grinenko, M. Abdel-Hafiez, S. Aswartham, M. Kumar, C. Hess, S. Wurmehl, K. Nenkov, A. U. B. Wolter, S.-L. Drechsler, and B. Büchner, e-print arXiv:1203.1585.

[21] H. Fukazawa, T. Saito, Y. Yamada, K. Kondo, M. Hirano, Y. Kohori, K. Kuga, A. Sakai, Y. Matsumoto, S. Nakatsuji *et al.*, J. Phys. Soc. Jpn. **80**, SA118 (2011).

[22] P. Popovich, A. V. Boris, O. V. Dolgov, A. A. Golubov, D. L. Sun, C. T. Lin, R. K. Kremer, and B. Keimer, Phys. Rev. Lett. **105**, 027003 (2010).

[23] G. Mu, H. Luo, Z. Wang, L. Shan, C. Ren, and H.-H. Wen, Phys. Rev. B **79**, 174501 (2009).

[24] A. K. Pramanik, M. Abdel-Hafiez, S. Aswartham, A. U. B. Wolter, S. Wurmehl, V. Kataev, and B. Büchner, Phys. Rev. B **84**, 064525 (2011).

[25] K. Hashimoto, A. Serafin, S. Tonegawa, R. Katsumata, R. Okazaki, T. Saito, H. Fukazawa, Y. Kohori, K. Kihou, C. H. Lee, A. Iyo, H. Eisaki, H. Ikeda, Y. Matsuda, A. Carrington, and T. Shibauchi, Phys. Rev. B **82**, 014526 (2010).

[26] H. Rosner *et al.* (to be published).

[27] S.-L. Drechsler, H. Rosner, M. Grobosch, G. Behr, F. Roth, G. Fuchs, K. Koepernik, R. Schuster, J. Malek, S. Elgazzar, M. Rotter, D. Johrendt, H.-H. Klauss, B. Büchner, and M. Knupfer, e-print arXiv:0904.0827 (2009).

[28] This estimate is based on the slightly higher experimental values of about 1.6 eV observed for less hole-doped samples [22,27] and the correspondingly slightly larger bare values from DFT calculations 2.63 to 2.7 eV. [27]

[29] V. G. Kogan, Phys. Rev. B **81**, 184528 (2010).

[30] Hussey, J. Phys. Soc. Jpn. **74**, 1107 (2005).

[31] A. C. Jacko, J. O. Hjarestadt, and B. J. Powell, Nat. Phys. **5**, 422 (2009).

[32] L. Boeri, O. V. Dolgov, and A. A. Golubov, Phys. Rev. Lett. **101**, 026403 (2008); L. Boeri, M. Calandra, I. I. Mazin, O. V. Dolgov, and F. Mauri, Phys. Rev. B **82**, 020506(R) (2010).

[33] H. Kawano-Furukawa, C. J. Bowell, J. S. White, R. W. Heskop, A. S. Cameron, E. M. Forgan, K. Kihou, C. H. Lee, A. Yyo, H. Eisaki, T. Saito, H. Fukazawa *et al.*, Phys. Rev. B **84**, 024507 (2011).

[34] K. Ohishi. Y. Ishii, H. Fukazawa, T. Saito, I. Watanabe, Y. Kohori, T. Suzuki, K. Kihou, C.-H. Lee, K. Miyazawa, H. Kito, A. Iyo, and H. Eisaki, e-print arXiv:1112.6078v1 (2011).

[35] S.-L. Drechsler, M. Grobosch, K. Koepernik, G. Behr, A. Kohler, J. Werner, A. Kondrat, N. Leps, C. Hess, R. Klingeler, R. Schuster, B. Büchner, and M. Knupfer, Phys. Rev. Lett. **101**, 257004 (2008).

[36] S.-L. Drechsler, F. Roth, M. Grobosch, R. Schuster, K. Koepernik, H. Rosner, G. Behr, M. Rotter, D. Johrendt, B. Büchner, and M. Knupfer, Physica C **470**, S332 (2010).

[37] The trivial case of a corresponding considerable number of electrons not involved in the superconducting condensate can be excluded by Eq. (6). In such a case $(n_s/n)2.64 = 2.28 = (1 + \lambda_{ph} + \lambda_{sf})(1 + \delta)$. Using even $\lambda_{ph} \sim 0.15$ for the remaining 75% of superconducting electrons, one is left with the same small disorder parameter $\delta = 1/3$ with $\lambda_{sf} \approx 0.3$ only, which is too small to explain the observed $T_c$ value as discussed. Only in the unrealistic absolute clean limit $\delta = 0$ would one be left with $\lambda_{sf} \approx 0.8$ and a reasonable $T_c$ value of 4–5 K. Therefore, a broad spectral Eliashberg function for the experimentally observed spin fluctuations centered at about 90.5 K[7] was used in our strong-coupling calculations.

[38] We stress that the small disorder adopted in the present analysis using Eqs. (5) and (6) is not applicable to our samples but only to the superclean sample of Ref. 33 for which the small penetration depth has been reported.

[39] J. A. Woollam, R. B. Somoano, and P. O. Connor, Phys. Rev. Lett. **32**, 712 (1974).

[40] C. K. Jones, J. K. Hulm, and B. S. Chandrasekhar, Rev. Mod. Phys. **36**, 74 (1964).

[41] M. R. Eskildsen, E. M. Forgan, and H. Kawano-Furukawa, Rep. Prog. Phys. **74**, 124504 (2011).

[42] H. Nakamura, M. Machida, T. Koyama, and N. Hamada, J. Jpn. Phys. Soc. **78**, 123712 (2009).

[43] N. R. Werthamer, E. Helfand, and P. C. Hohenberg, Phys. Rev. **147**, 295 (1966).

[44] V. Grinenko, K. Kikoin, S.-L. Drechsler, G. Fuchs, K. Nenkov, S. Wurmehl, F. Hammerath, G. Lang, H.-J. Grafe, B. Holzapfel,

J. van den Brink, B. Büchner, and L. Schultz, Phys. Rev. B **84**, 134516 (2011).

[45] A. Gurevich, Phys. Rev. B **67**, 184515 (2003).

[46] A. Gurevich, Rep. Prog. Phys. **74**, 124501 (2011).

[47] C. Tarantini, A. Gurevich, J. Jaroszynski, F. Balakirev, E. Bellingeri, I. Pallecchi, C. Ferdeghini, B. Shen, H. H. Wen, and D. C. Larbalestier, Phys. Rev. B **84**, 184522 (2011).

[48] Starting with the BCS expression for the Pauli-limiting field for a $d$-wave superconductor $2.25T_c = 6.3$ T (which is somewhat smaller than the WHH-orbital field of 7.37 T) and using the experimental data of Terashima *et al.*,[4] one concludes that for their sample the paramagnetic pair breaking should in fact play some role. However, these data can be fitted alternatively with a significantly smaller Maki parameter $\alpha$ and with a nearly isotropic spin-orbit coupling constant. (Our full relativistic band structure calculation predicts a 10% change both for the mass anisotropy and for the Fermi velocities as compared with usually employed scalar relativistic ones.) One then extrapolates $\mu_0 H_{c2,ab}^*(0) = 7.0$ T for $\lambda_{so} = 0.1$, $\alpha = 1.4$, and the Pauli-limited field of $\mu_0 H_{c2,ab} = 4.4$ T. Therefore, the fitted slope for the $(ab)$ direction is slightly reduced to $-3.6$ T/K, which seems to be still within the error bars of the slope of $-3.8$ T/K reported there. Thus, we arrive at a slope anisotropy near $T_c$ of 5.07 instead of 6.8 as claimed in Ref. 4 and very close to our value of 5.05 reported above. The obtained empirical Pauli limiting field of 6.25 T is very close to the $d$-wave BCS estimate given above, which points again to a weak-coupling scenario. Thus, in our intepretation of the data of Ref. 4, the anisotropy at $T = 0$ is reduced to 3.68 due to Pauli limiting. We ascribe that Pauli-limiting behavior, absent in our cleaner samples, to an enlarged concentration of magnetic moments involved in the pair-breaking subsystem that enhances the effective Pauli susceptibility in governing the paramagnetic effect according to the Wolff mechanism.[44]

[49] Y. Jia, P. Cheng, L. Fang, H. Luo, H. Yang, C. Ren, L. Shan, C. Gu, and H.-H. Wen, Appl. Phys. Lett. **93**, 032503 (2008).

[50] J. J. Hamlin, R. E. Baumbach, D. A. Zocco, T. A. Sayles, and M. B. Maple, J. Phys.: Condens. Matter **20**, 365220 (2008).

[51] U. Welp, R. Xie, A. E. Koshelev, W. K. Kwok, H. Q. Luo, Z. S. Wang, G. Mu, and H. H. Wen, Phys. Rev. B **79**, 094505 (2009).

[52] H. Q. Yuan, J. Singleton, F. F. Balakirev, S. A. Baily, G. F. Chen, J. L. Luo, and N. L. Wang, Nature **457**, 565 (2009).

[53] E. Backen, S. Haindl, T. Niemeier, R. Hühne, J. Freudenberg, J. Werner, G. Behr, L. Schultz, and B. Holzapfel, Supercond. Sci. Technol. **21**, 122001 (2008).

[54] J. Bardeen, L. N. Cooper, and J. R. Schrieffer, Phys. Rev. **108**, 1175 (1957).

[55] K. Deguchi, Z. Q. Mao, H. Yaguchi, and Y. Maeno, Phys. Rev. Lett. **92**, 047002 (2004).

[56] K. Naoyuki *et al.*, J. Phys. Soc. Jpn. **79**, 113702 (2010).

[57] F. Hardy, T. Wolf, R. A. Fisher, R. Eder, P. Schweiss, P. Adelmann, H. Löhneysen, and C. Meingast, Phys. Rev. B **81**, 060501(R) (2010).

[58] I. I. Mazin, D. J. Singh, M. D. Johannes, and M. H. Du, Phys. Rev. Lett. **101**, 057003 (2008).

[59] M. Yashima, H. Nishimura, H. Mukada, Y. Kitaoka, K. Miyazawa, P. M. Shirage, K. Kihou, H. Kito, H. Eisaki, and A. Iyo, J. Phys. Soc. Jpn. **78**, 103702 (2009).

[60] Z. Shermadini, J. Kanter, C. Baines, M. Bendele, Z. Bukowski, R. Khasanov, H.-H. Klauss, H. Luetkens, H. Maeter, G. Pascua, B. Batlogg, and A. Amato, Phys. Rev. B **82**, 144527 (2010).

[61] F. Bouquet, Y. Wang, R. A. Fisher, D. G. Hinks, J. D. Jorgensen, A. Junod, and N. E. Phillips, Europhys. Lett. **56**, 856 (2001).

[62] B. Mühlschlegel, Z. Phys. **155**, 313 (1959).